7.9 OBSERVATIONS OF COUPLING BETWEEN WIND STRESS AND SEA SURFACE TEMPERATURES AT MID-LATITUDES

Larry W. O'Neill and Dudley B. Chelton
College of Oceanic and Atmospheric Sciences
Oregon State University, Corvallis, Oregon

1. INTRODUCTION

Several previous studies have documented the relationship between sea surface temperature (SST) gradients and surface winds. The vertical transfer of momentum is affected by the changing SST and has a controlling effect on the surface wind magnitude.Sweet et al. (1981) noted that wind speeds at 61 m elevation were nearly 5 m s^{-1} less over the cold side of the Gulf Stream than over the warm side. Over the northern Agulhas Current near 37S and 20E, Jury and Walker (1988) found an increase in wind speed of nearly 7 ms^{-1} across the SST front. Using aircraft observations across the warm Agulhas Current near 35S and 23E, Jury (1993) found that across an SST front of 8 deg C, surface wind stress increased by a factor of 5 toward the warmer waters. From an analysis of climatological data in the eastern tropical Pacific, Wallace et al. (1989) hypothesized that surface winds decouple from winds aloft as air blows from warm to cold water due to an increase in static stability, causing the surface winds to decrease. Conversely, winds that blow from colder to warmer waters are coupled with the winds aloft due to turbulence generated by the surface heating of the atmospheric boundary layer. In this case, the wind speed will increase across the SST front because turbulence will transfer higher momentum from aloft downwards to the surface.

From sparse mooring observations, Hayes et al. (1989) presented evidence for a coupling between surface winds and SST on monthly time scales in association with tropical instability waves (TIW's) in the eastern Pacific. Xie et al. (1998) found more evidence of coupling from satellite observations of SST and wind observations from the NASA scatterometer (NSCAT). Clear evidence of the effects of TIW-induced pertubations of SST on the overlying wind field has recently been presented by Chelton et al. (2001). Using wind stress measurements obtained from the QuikSCAT scatterometer, Chelton et al. (2001) found positive, linear relationships between the wind stress divergence and curl and the downwind SST gradient and crosswind SST gradient, respectively, over the TIW's in the eastern Pacific.

2. METHODS

This study further characterizes the relationship between SST gradients and surface wind fields by extending the methods of Chelton et al. (2001) from the tropics to mid-latitudes. Specifically, results are presented from the Southern Ocean along the entire Antarctic Circumpolar Current (ACC), from 40S latitude to 57S latitude. At these latitudes, the annual mean wind direction is nearly zonal, blowing from west to east. The mean zonally averaged curl is positive and steadily increases from low latitudes to a maximum near 45S at which point it decreases southward towards the Antarctic coast. This large-scale curl is associated with the mid-latitude westerly wind jet of the Southern Hemisphere.

The surface wind stress was measured by the SeaWinds scatterometer aboard the QuikSCAT satellite launched on 19 June 1999 (Freilich et al. 1994). The data record used here is from the 11-month period of July 21, 1999 to June 28, 2000. For this study, a mean field is constructed for the entire time period and then analyzed. The scatterometer infers surface vector wind stress over water from measurements of microwave radar backscatter. The winds are calibrated to the neutral stability wind at a height of 10 m above the sea surface. The relation between the neutral wind vector at 10 m $\mathbf{v_{10}}$ and the wind stress vector $\boldsymbol{\tau}$ is related by $\boldsymbol{\tau} = \rho C_{dN} \mathbf{v_{10}} |\mathbf{v_{10}}|$, where ρ is the air density, and C_{dN} is the neutral stability drag coefficient (Large and Pond 1981). Further considerations of the QuikSCAT data used in this study are discussed in Chelton et al. (2001).

The SST used in this study are from the observation-based weekly-average Reynolds analyses (Reynolds 1994). Over the Southern Ocean, most of the measurements of SST are from ships, buoys and occasional AVHRR measurements when clouds are not present. In the Southern Ocean in particular, the SST fields may contain significant systematic sampling errors due to sparse measurements. However, the Reynolds analyses are one of the few SST products available for this part of the world and are found to be adequate for the purposes used here. The SST fields averaged over the same 11-month period as the QuikSCAT data do resolve several permanent standing meanders that exist in the ACC due to topographic features in the flow (Colton and Chase, 1983; Chelton et al. 1990). It is shown here that these meanders in the SST fields produce characteristic features in the derivative wind fields.

To evaluate how the SST field affects the wind stress curl, it is necessary to remove the large scale curl signal, as the pertubations to the surface wind field

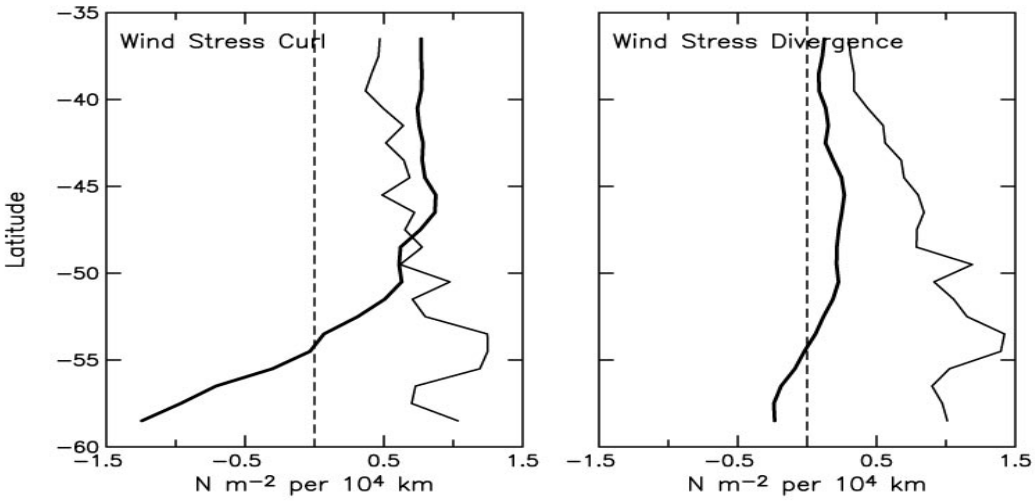

Figure 1. The left panel shows the zonally averaged wind stress curl fields (heavy solid curve) and the standard deviation of the zonal curl field (thin solid curve). The right panel shows the zonally averaged divergence (heavy solid curve) and the standard deviation of the zonal divergence field (thin solid curve).

induced by the SST gradients are otherwise difficult to distinguish. Figure 1 shows a plot of the zonally averaged wind stress curl and divergence fields over the entire 11-month period. The heavy solid curve in both plots is the zonal mean and the thin solid curve is the zonal standard deviation of the wind stress curl and divergence. The mean zonally averaged curl signal is larger than the standard deviation over the northern ACC SST front, indicating that the background mean curl signal is larger than the variability in the signal. This background curl signal will mask the SST-induced pertubations that are being studied here, making it necessary to somehow remove this background signal.

To accomplish this, the wind stress curl fields were spatially high-passed filtered to remove the synoptic and mesoscale meteorological processes that have spatial scales longer than the scales of the SST-induced pertubations in the surface wind field. The filtered derivative wind fields allow an investigation of the influence of the SST gradients operating on smaller dimensional scales. The half-width of the high-pass filter is 30 degrees of longitude and 20 degrees of latitude. The results of this study are not seen to be particularly sensitive to choices in the filtering parameters.

The wind stress divergence fields have a small zonal mean compared to the standard deviation. Spatial high-pass filtering of these fields is not necessary to identify SST-induced pertubations of the wind stress divergence but is done to keep the analysis consistent between the curl and the divergence. The results obtained here are almost identical using the filtered or unfiltered divergence fields.

The pertubation downwind SST gradient is the component of ∇T given by the vector dot product $(\nabla T \bullet \boldsymbol{\tau})'$, where T is the SST and $\boldsymbol{\tau}$ is a unit vector pointing in the direction of the pertubation wind stress. The crosswind SST gradient is $(\nabla T \times \boldsymbol{\tau})'$.

3. RESULTS

The top panel in Figure 2 shows a histogram of the downwind SST gradient observations. The observations are symmetrically distributed with a zero mean indicating that there is no preference in the pertubation fields for wind blowing towards warmer or cooler waters. The bottom panel in Figure 2 shows the binned observations of pertubation wind stress divergence against the pertubation downwind SST gradient. It is evident from the linear relation that positive (negative) pertubations in the downwind SST gradient produce pertubation divergence (convergence) in the surface wind stress fields.

The histogram of the pertubation crosswind SST gradient is shown in the top panel in Figure 3. These observations are approximately symmetrically distributed with a zero mean. Similar to the wind stress divergence, the binned observations of the pertubation wind stress curl versus the pertubation crosswind SST gradient also show a linear relation.

These linear relations indicate that the pertubation wind stress divergence and curl depend, respectively, on the cosine and sine of the pertubation angle defined by $\theta' = \tan^{-1} [(\nabla T \times \tau)' / (\nabla T \bullet \tau)']$. Figure 4 shows a histogram of the pertubation angle. The bottom two panels show, respectively, the binned observations of

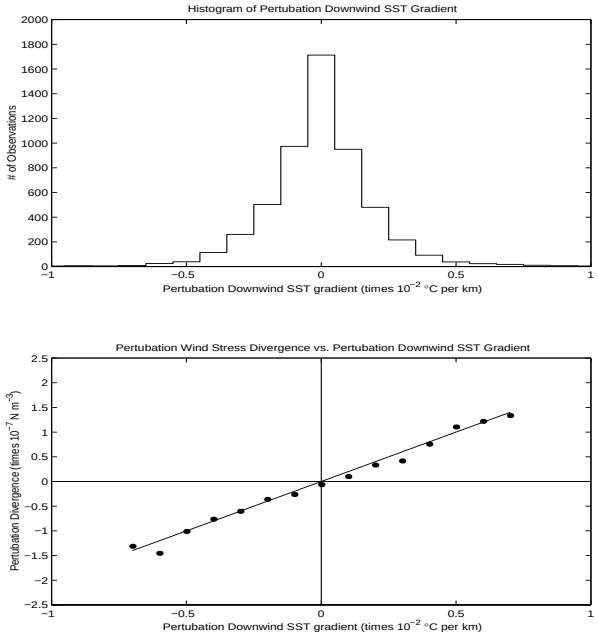

Figure 2. The top panel shows a histogram of the circumpolar 1° gridded observations of the pertubation downwind SST gradient between 40S-57S latitude. There are 5,531 grid points over this region. The bottom panel shows the binned observations of the pertubation wind stress divergence against the pertubation downwind SST gradient.

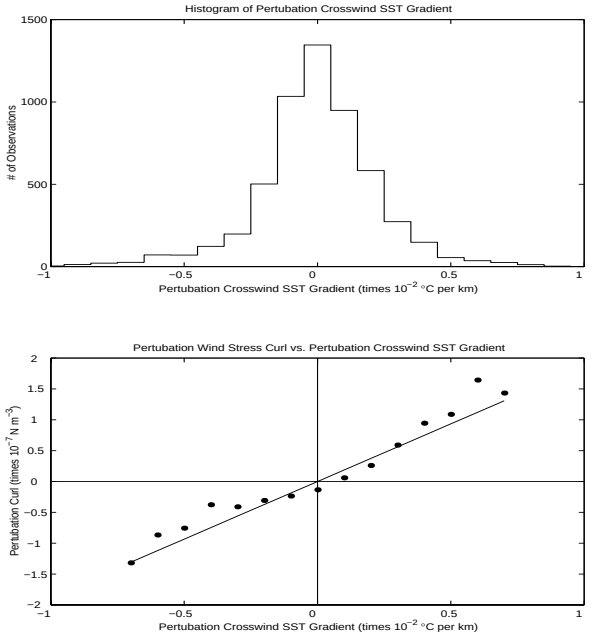

Figure 3. The top panel shows a histogram of the circumpolar 1° gridded observations of the pertubation crosswind SST gradient between 40S-57S latitude. There are 5,497 grid points over this region. The bottom panel shows the binned observations of the pertubation wind stress divergence against the pertubation downwind SST gradient.

the pertubation wind stress divergence and curl versus the pertubation angle θ′. The smooth curves are least-squares fits of cosine and sine curves to the binned data. The results for both the divergence and curl show very good agreement between the expected cosine and sine dependencies. On the time and space scales presented here, these results confirm the hypothesized dependencies of the wind stress divergence and curl fields on the orientation of the wind stress vector relative to the underlying SST gradient.

Each of the linear relations of the divergence and curl were fitted to a least-squares straight line for bins that have more than 40 observations. The slope of the line for the pertubation divergence is 0.020 N m^{-2} $°C^{-1}$ and that of the pertubation curl is 0.019 N m^{-2} $°C^{-1}$. Comparing these slopes with what Chelton et al. (2001) obtained for the eastern tropical Pacific shows that the slopes obtained here in the Southern Ocean are very nearly the same.

Wind divergence and curl have significant dynamical influences and it would be interesting to see what the dynamical consequences of this coupling between SST and wind stress are for both the ocean and the lower atmosphere. Certainly regions of preferential curl or divergence that are evident from a yearly mean such as this analysis has used must have some significant local response to this forcing.

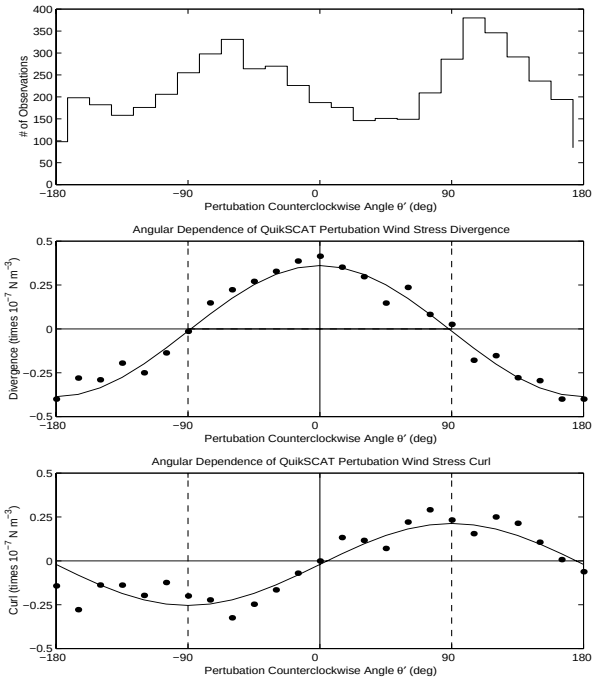

Figure 4. The top panel shows a histogram of the observations of the counterclockwise pertubation angle. There are 5,497 grid points over this region. The middle panel shows the binned angular dependence of the pertubation wind stress divergence. The solid curve is a least-squares fit of a cosine to the binned data. The bottom panel shows the binned angular dependence of the pertubation wind stress curl. The solid curve is a least-squares fit of a sine to the binned data.

Further work includes looking to see if this coupling occurs over the Gulf Stream and Kuroshio Extension and to see if there are any differences from the responses found in the eastern tropical Pacific and the Southern Ocean.

REFERENCES

Chelton, D. B., S. K. Esbensen, M. G. Schlax, N. Thum, M. H. Freilich, F. J. Wentz, C. L. Gentemann, M. J. McPhaden and P. S. Schopf, 2001: Observations of coupling between surface wind stress and sea surface temperature in the Eastern Tropical Pacific. *J. Climate*, In Press.

Chelton, D. B., M. G. Schlax, D. L. Witter and J. G. Richman, 1990: Geosat altimeter observations of the surface circulation of the Southern Ocean. *J. Geophys. Res.,* **95**(C10), 17887-17903.

Colton, M. T. and R. R. P. Chase, 1983: Interaction of the Antarctic Circumpolar Current with bottom topography: An investigation using satellite altimetry. *J. Geophys. Res.,* **88**(C3), 1825-1843.

Hayes, S. P., M. J. McPhaden and J. M. Wallace, 1989: The influence of sea-surface temperature on surface wind in the eastern equatorial Pacific: Weekly to monthly variability. *J. Clim.,* **2**, 1500-1506.

Jury, M. R., 1993: A thermal front within the marine atmospheric boundary layer over the Agulhas Current south of Africa: Composite aircraft observations. *J. Geophys. Res.*, **99**(C2), 3297-3304.

Jury, M. R., N. Walker, 1988: Marine boundary layer modification across the edge of the Agluhas Current. *J. Geophys. Res.,* **93**(C1), 647-654.

Sweet, W., R. Fett, J. Kerling and P. LaViolette, 1981: Air-sea interaction effects in the lower troposphere across the north wall of the Gulf Stream. *Mon. Weather Rev.*, **109**, 1042-1052.

Wallace, J. M., T. P. Mitchell and C. Deser, 1989: The influence of sea-surface temperature on surface wind in the Eastern Equatorial Pacific: seasonal and interannual variability. *J. Climate*, **21**, 1492-1499.

Xie, S.-P., M. Ishiwatari, H. Hashizume and K. Takeuchi, 1998: Coupled ocean-atmospheric waves on the equatorial front. *Geophys. Res. Lett.*, **25**, 3863-3866.

Corresponding author address: Larry W. O'Neill, College of Oceanic and Atmospheric Sciences, Oregon State University, 104 Ocean Admin. Bldg., Corvallis, OR 97330